An Enhanced Virtual Impedance Optimization Method for Reactive Power Sharing in Microgrids

Yixin Zhu, *Member, IEEE*, Qigao Fan, *Member, IEEE*, Baoquan Liu, *Member, IEEE*, and Tao Wang

***Abstract*—To solve the reactive power sharing issue of the conventional droop control method, communication is commonly used, especially in networked microgrids. However, there are still many occasions where communication has not been established in advance. In such cases, the wireless reactive power sharing strategy based on the virtual impedance optimization can be applied. By designing and optimizing the controller of virtual impedance, the global reactive power sharing error of the microgrid can be minimized. Thus, the reactive power sharing performance of the droop control method is improved accordingly. However, the original optimization method has not considered the different capacities of distributed generation (DG) units, and it is subject to the number of network nodes. In this paper, an enhanced virtual impedance optimization method is proposed to solve the two issues. First, the reactive power estimation method used in the fitness function is modified to adapt to the system that contains DG units with different capacities. Second, a network simplification step is added before the optimization to deal with the system with more nodes. With these improvements, the application scope of the virtual impedance optimization method is greatly extended. Finally, the effectiveness of the enhanced method is verified through a 38-bus system in MATLAB simulation.**

***Index Terms*—Droop control, networked microgrid, optimization problem, reactive power sharing, virtual impedance.**

I. Introduction

THE microgrid, as a small-scale power system, has the capability to increase the penetration of distributed generations (DG) into the main grid [1]. It can operate in either grid-connected mode or islanded mode, thereby improving the power supply reliability for the end user. The microgrid provides an efficient integration solution for distributed energy resources and distributed energy storage systems. So far, the microgrid has been widely studied and a variety of surveys have been reported, particularly on the subject of architectural, stability analysis, power quality improvement, power sharing, energy management, etc.

For the islanded microgrid, load power must be properly shared among multiple DG units. If economic factors are not considered, DG units should output power in proportion to their power capacities. To achieve this, the frequency and voltage magnitude droop control method is commonly used, which mimics the behavior of synchronous machines in the power system [2], [3]. The droop control manner is completely distributed, making the microgrid operation independent of communication links. The wireless control manner enables the "plug and play" function of DG units and also enhances the reliability of the system. Although the frequency droop control can realize accurate real power sharing, the voltage magnitude droop control typically results in poor reactive power sharing due to the mismatch in line impedances and local loads [4]. Moreover, when the microgrid structure is networked, the reactive power sharing issue will be trickier.

To improve the reactive power sharing performance of the droop control method, many solutions have been developed. Among these solutions, the virtual impedance method, as an efficient supplementary means for the droop control method, is frequently used. In [5] and [6], predominant virtual inductors are added to DG units, which can compensate the mismatch in line impedances to some extent, thereby reducing some reactive power sharing errors. However, the main target is to prevent the instability of power control. In [7]–[9], virtual impedances are designed to compensate the mismatch in the output impedances of the closed-loop controlled DG units. But for a microgrid system, the reactive power sharing issue is not only caused by the internal factors of DG units. In [10]–[12], the impacts of the mismatched line impedances and local loads on reactive power sharing are considered. In [10], reactive power sharing errors are eliminated through the modification of droop control slopes. To enhance the effect, communication is then introduced to help estimating the line impedance [11]. In [12], by associating feeder current with the virtual impedance control, the transient process after load change becomes faster and more stable. However, the above-mentioned methods have some requirements in the microgrid structure: all the DG units need to connect directly to the common ac bus. So, when the microgrid has a networked structure, these methods cannot work properly as desired.

To solve the reactive power sharing issue in networked microgrids, the communication-based solution becomes a shortcut. Synchronizing signals are utilized in [13]–[15] to trigger an extra regulation process for reactive power sharing, but the control

Manuscript received October 14, 2017; revised January 17, 2018; accepted February 20, 2018. Date of publication February 28, 2018; date of current version September 28, 2018. This work was supported in part by the Operation Fund of Guangdong Key Laboratory of Clean Energy Technology under Grant 2014B030301022 and in part by the Fundamental Research Funds for the Central Universities under Grant JUSRP11741. Recommended for publication by Associate Editor Li Zhang. *(Corresponding author: Yixin Zhu.)*

Y. Zhu, Q. Fan, and T. Wang are with the School of Internet of Things, Jiangnan University, Wuxi 214122, China (e-mail: zhuyixin1987@163.com; qgfan@jiangnan.edu.cn; 568256052@qq.com).

B. Liu is with the School of Electrical and Information Engineering, Shaanxi University of Science and Technology, Xi'an 710021, China (e-mail: liubq@sust.edu.cn).

Color versions of one or more of the figures in this paper are available online at http://ieeexplore.ieee.org.

Digital Object Identifier 10.1109/TPEL.2018.2810249

See http://www.ieee.org/publications_standards/publications/rights/index.html for more information.

performance is easy to be influenced if loads change during the regulation period. When data communication is set up between the microgrid central controller and DG units, accurate reactive power sharing can be achieved through the centralized control manner, either by tuning the virtual impedances or the Q–V set points [16]–[20]. In recent years, the control methods based on the multi-agent consensus protocol have been also developed, which can realize accurate reactive power sharing by only using a sparse communication network [21]–[24]. Differing from the centralized control manner, the consensus-based control methods are highly distributed, as DG units only communicate with their neighbor units. By this means, the microgrid system is easier to be expanded. Not only that, when communication is utilized, the voltage deviation issue of the droop control can also be solved [25]–[27].

Although communication can help improve the reactive power sharing performance of the droop control method, there are still many occasions where communication has not been built due to economic or geography reasons. In such cases, the wireless solution can still be the first choice. However, most wireless methods cannot provide satisfactory reactive power sharing performance for the networked microgrid. In [28], a wireless reactive power sharing strategy based on the virtual impedance optimization method is proposed for the networked microgrid: by designing and optimizing the controller of virtual impedance, the global reactive power sharing error of a microgrid can be minimized and limited to a low level. Thus, the reactive power sharing performance of the droop control method is improved accordingly. The technical details of the virtual impedance optimization method are as follows.

1) When the virtual impedance optimization method is applied, DG units do not need any hardware update. So, it can easily help the existing microgrid improve the reactive power sharing performance.
2) The only difference is that a specially designed virtual impedance controller is added to each DG unit. Through the adaptive virtual impedances, the reactive power sharing errors of a microgrid can be limited to a low level.
3) According to the network parameters and voltage level, the relationship between the virtual impedance and output power is derived and analyzed. Then, the controller expression of virtual impedance can be determined.
4) In the controller expression, virtual impedance and output power are correlated, but the detailed controller parameters are undetermined. Normally, DG units have individual controller parameters, due their different locations and capacities.
5) To obtain the exact controller parameters, an optimization problem based on the global reactive power sharing error is designed. The core of building the fitness function is an estimation method, which estimates the reactive power sharing error of a given network.
6) In the optimization, the microgrid is assumed to operate under different operation points, each of which corresponds to a network. By accumulating the reactive power sharing error of each operation point, the global reactive power sharing error of the microgrid can be obtained.
7) The calculation function of the global reactive power sharing error is then set as the fitness function to further build the optimization problem. And the undetermined parameters of the virtual impedance controllers are all set as the optimization variables.
8) By using the genetic algorithm, the optimization problem can be well solved. The obtained controller parameters, as the optimal solution for the optimization problem, are then configured to the corresponding DG units.

The optimization method enables wireless reactive power sharing control among DG units. However, the original method has not considered the different capacities of DG units, and it is subject to the number of network nodes. As the node number increases, the calculation amount of the optimization problem solving will become massive, making the optimization method invalid. So, two improvements are made in this paper.

1) By incorporating reactive power droop slopes into the calculation formulae, the reactive power estimation method used in the fitness function is modified to adapt to the system containing DG units with different capacities.
2) By rationally simplifying the network of the microgrid, the number of microgrid operation points is greatly reduced, making the virtual impedance optimization method not subject to the network node number.

Through the two improvements, the improved method can have a much wider application scope compared with the original method. But it should be noted that, due to the lack of communication, the optimization method can hardly add secondary regulation function to control the voltage.

This paper is organized as follows. The reactive power sharing strategy based on the virtual impedance optimization method is introduced in Section II. Section III presents the modified reactive power estimation method, which takes account of the different capacities of DG units. The network simplification is discussed in Section IV. In Section V, some simulation results are given to validate the improved virtual impedance optimization method. Conclusions are finally drawn in Section VI.

II. Reactive Power Sharing Strategy Based on the Virtual Impedance Optimization Method

A. Reactive Power Sharing Issue of the Conventional Droop Control Method

With the fast development of microgrids, more and more "plug and play" DG units are applied to the system. This trend leads to some changes in the structure of the traditional microgrid and forms the networked microgrid, as shown in Fig. 1. In the networked microgrid, DG units can be connected to any node of the network. The loads connected directly to DG unit nodes are local loads, and the others are public loads. Considering that the focus of this paper is the fundamental real and reactive power control, nonlinear loads are assumed to be limited in the microgrid. Like the traditional microgrid, by controlling the static transfer switch at the point of common coupling, the networked microgrid can also operate in either islanded mode or grid-connected mode. In the grid-connected mode, as the voltage of the microgrid is supported by the main grid, power

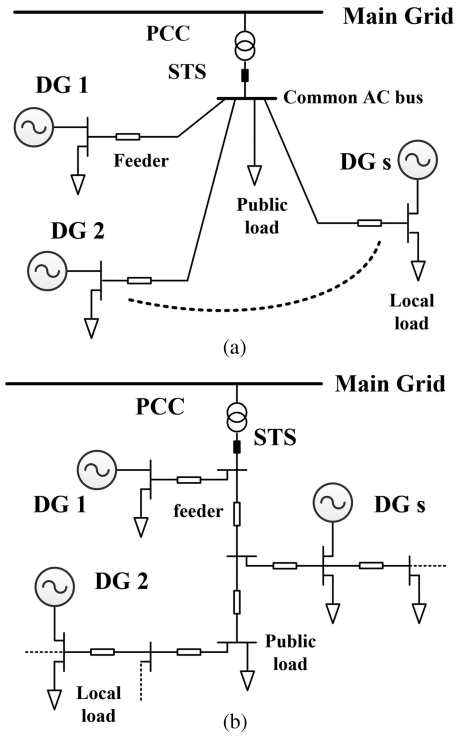

Fig. 1. Different structures of the microgrid. (a) Traditional structure. (b) Networked structure.

sharing can be easily realized by adopting power tracking techniques. However, in the islanded mode, power sharing relies on the cooperation of multiple DG units.

Normally, for an islanded microgrid, DG units can employ the conventional real power–frequency droop control and reactive power–voltage magnitude droop control as

$$f_i^* = f_0 - D_{pi}P_i \tag{1}$$

$$E_i^* = E_0 - D_{qi}Q_i \tag{2}$$

where f_0 and E_0 are the initial frequency and voltage magnitude of the DG unit, respectively; P_i and Q_i are the measured real and reactive powers after the first-order low-pass filtering, respectively; and D_{pi} and D_{qi} are the real and reactive power droop slopes of DG i, respectively. Normally, they are associated with the power capacity of the DG unit, which can be defined as

$$D_{pi} = \frac{f_{\max} - f_{\min}}{P_{\max i}} \tag{3}$$

$$D_{qi} = \frac{E_{\max} - E_{\min}}{Q_{\max i}} \tag{4}$$

where $f_{\max}$ and $f_{\min}$ are the upper and lower bounds of the microgrid frequency, respectively; $E_{\max}$ and $E_{\min}$ are the upper and lower bounds of the voltage magnitude, respectively; and $P_{\max i}$ and $Q_{\max i}$ are the real and reactive power capacities of DG i. With the derived frequency and voltage magnitude, the instantaneous voltage reference can be obtained accordingly.

According to (3) and (4), the droop slopes are inversely proportional to the DG capacities. Normally, DG units with larger capacities will be set with smaller droop slopes, and vice versa. So that when all the DG units operate under the same frequency and voltage magnitude, the larger DG units could output more real and reactive powers according to (1) and (2). In practice, due to the consistent frequency among DG units, the P–ω droop control can easily achieve accurate real power sharing. However, as the voltage magnitudes of DG units can hardly be unified due to the mismatch in network parameters, the Q–V droop control always suffers reactive power sharing issues. For a low-voltage microgrid, where distribution feeders are mainly resistive, the P–V and Q–f droop control method can be used. This inverse droop control can achieve an accurate reactive power sharing state. Instead, it has real power sharing issues. Considering that the real power is associated with the energy consumption, the conventional droop control method is selected as the basic control here. In traditional microgrids, reactive power sharing errors are mainly caused by the mismatch in line impedances and local loads. By adding some local control, the reactive power sharing issue can be solved without using communication [10]–[12]. However, due to the irregular distribution of DG units, communication becomes essential for networked microgrids. But the introduction of communication also results in some new issues, such as cost increase and equipment upgrading. Then, the virtual impedance optimization method based reactive power sharing strategy can be applied for networked microgrids [28].

B. Proposed Reactive Power Sharing Strategy

As a supplementary means for the droop control method, the virtual impedance technique can improve both the control stability and reactive power sharing performance of the system. Normally, the value of virtual impedance is fixed, which is simple but not efficient. However, as the load changes in the microgrid, the input impedance of each DG unit will change accordingly. To realize tracing compensation, it would be better if the virtual impedance has regulating ability. In [28], reactive power sharing control is realized through several specially designed virtual impedance controllers. The diagram of the networked microgrid using the proposed control strategy is illustrated in Fig. 2.

As can be seen from the figure, the DG units in the microgrid are fully distributed. Each DG unit is equipped with an individual virtual impedance controller. As mentioned before, these controllers have different parameters, which are obtained by solving the optimization problem. As the microgrid operates, the controller will generate virtual impedance reference for its local DG unit according to the power change. Through the cooperation of these optimized virtual impedance controllers, DG units can well share the load power.

C. Workflow of the Virtual Impedance Optimization Method

The virtual impedance optimization method is offline used, as shown in Fig. 2. Before it works, the microgrid staff needs to collect some necessary network information, such as the network topology, line impedances, and the load range of each node. The workflow of the virtual impedance optimization method is briefly illustrated in Fig. 3.

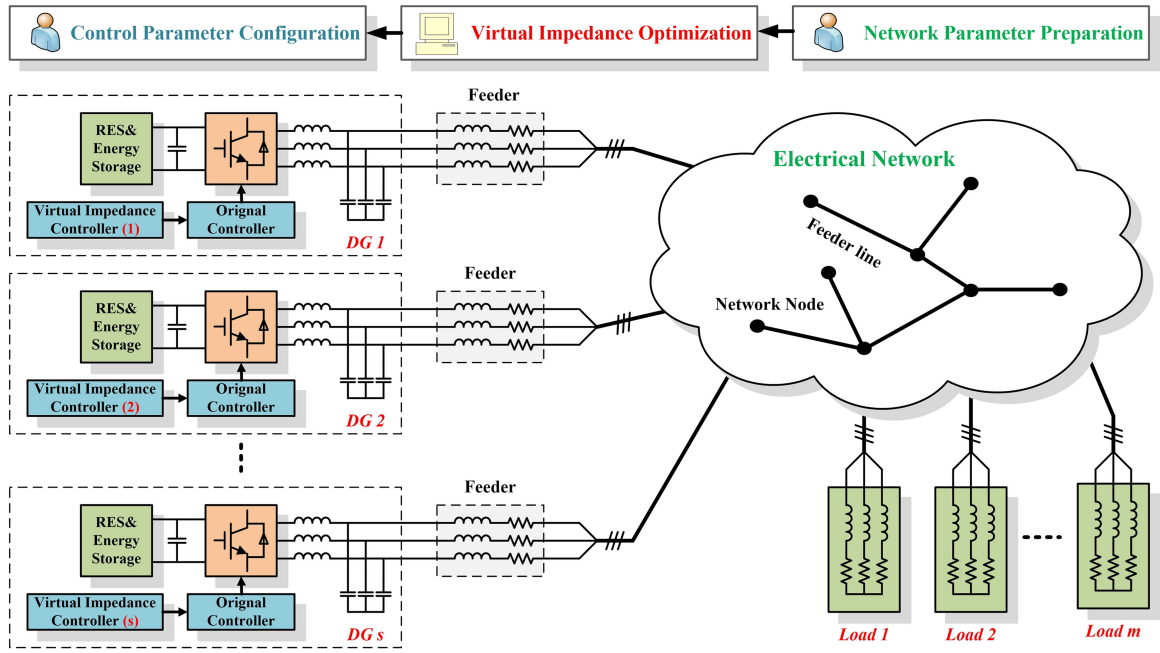

Fig. 2. Overview for the virtual impedance optimization method based reactive power sharing strategy.

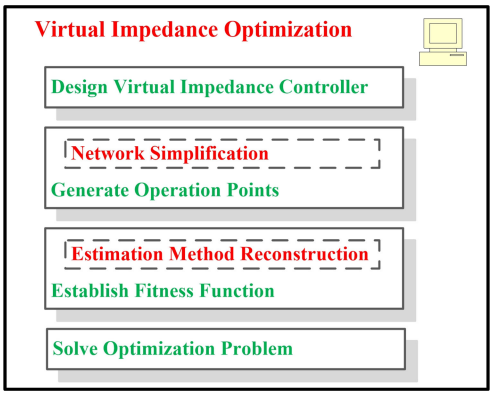

Fig. 3. Main steps of the virtual impedance optimization method.

As the figure shows, the virtual impedance optimization method mainly contains four steps. First, determine the controller expression for virtual impedance, with the controller parameters undetermined. Second, set the operation points for single load to further generate the complete microgrid operation points. Third, establish the calculation function of the global reactive power sharing error based on the reactive power estimation method. Finally, set the calculation function as the fitness function and then solve the optimization problem to obtain the specific controller parameters.

In the designed virtual impedance controller, the virtual reactance is fixed to a large value to maintain the system stability, while the virtual resistance is adjustable for reactive power regulation. The virtual resistance is controlled by the output power. When a local load is included, the power of the local load can also be added to the controller expression. In the optimization, the microgrid is assumed to operate at many different microgrid operation points. A microgrid operation point is composed of load operation points. If the microgrid contains m loads and each load has k operation points, there will be total k^m operation points for the microgrid, each of which corresponds to a specific network. It should be noted that the load operation points are not actual, which are set artificially according to the power range of load. In the calculation function, the parameters of the virtual impedance controllers are designed as the inputs, and the output is the global reactive power sharing error. With the proposed estimation method, the reactive power sharing error of a single microgrid operation point can be calculated. By accumulating the reactive power sharing error of each microgrid operation point, the global reactive power sharing error can be obtained. Finally, with the optimized controllers, DG units can well share the reactive power during the operation stage of the microgrid. As the load network is linear, as long as the load operates in the designed range, the reactive power sharing errors will be limited. It can be seen that the whole optimization process is completed offline, where communication is not required.

However, the original method has not considered the different capacities of DG units, and it is subject to the number of network nodes. To solve these issues, network simplification is added in step 2; meanwhile, the reactive power estimation method used in step 3 is improved.

III. Improved Reactive Power Estimation Method

A. Original Reactive Power Estimation Method

To control the calculation amount of the fitness function, the reactive power estimation method, as the core of the global reactive power sharing error calculation, should be simple and efficient. In [28], by ignoring the voltage differences of DG

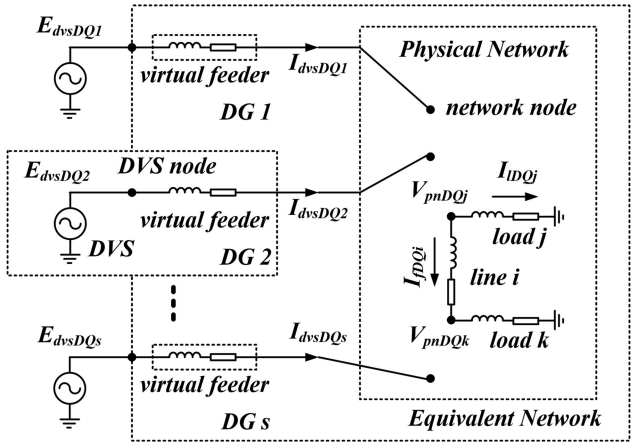

Fig. 4. Sketch of the networked microgrid model.

units, the reactive power sharing error of a microgrid operation point can be estimated. The main processes are as follows.

1) Microgrid Model and Admittance Matrix: A conceptual microgrid model is established in a *D–Q* synchronous rotating reference frame, as shown in Fig. 4. In the figure, the dashed part indicates the equivalent network of the microgrid, containing a physical network and several virtual feeders. The whole microgrid system is composed of a physical network and *s* DG units. Considering that DG units with the *PQ* control can be treated as special loads, they are not discussed in this study. In the presented model, all the DG units apply the droop control method. When the virtual impedance method is applied, the DG unit can be equivalent to a droop-controlled voltage source (DVS) in series with a virtual feeder. By separating these DVS units, the equivalent network of the microgrid can be obtained.

In the microgrid model, there are total *s* DG units, *n* network feeders, and *m* network nodes. With the parameters of the line impedances, virtual impedances, and load impedances, the admittance matrix $\mathbf{Y}_{\text{net}}$ of the equivalent network can be derived. The detailed derivation process of $\mathbf{Y}_{\text{net}}$ can be found in [28], and its final form is as follows:

$$\mathbf{Y}_{\text{net}} = \begin{bmatrix} \mathbf{Y}_{11} & \mathbf{Y}_{12} & \cdots & \mathbf{Y}_{1s} \\ \mathbf{Y}_{21} & \mathbf{Y}_{22} & \cdots & \mathbf{Y}_{2s} \\ \vdots & \vdots & \ddots & \vdots \\ \mathbf{Y}_{s1} & \mathbf{Y}_{s2} & \cdots & \mathbf{Y}_{ss} \end{bmatrix}_{2s\times 2s} \tag{5}$$

where

$$\mathbf{Y}_{ij} = \begin{bmatrix} G_{ij} & -B_{ij} \\ B_{ij} & G_{ij} \end{bmatrix}.$$

In (5), $\mathbf{Y}_{\text{net}}$ is expressed as a partition matrix. Its diagonal submatrix $\mathbf{Y}_{ii}$ represents the input admittance of DVS *i*, which reflects the network port characteristics. The off-diagonal submatrices $\mathbf{Y}_{ij}$ and $\mathbf{Y}_{ji}$ reflect the coupling between DVS *i* and *j*, which are always equal. Thus, the admittance matrix $\mathbf{Y}_{\text{net}}$ is a partition symmetric matrix.

2) Reactive Power Estimation: With the derived admittance matrix $\mathbf{Y}_{\text{net}}$, the *DQ*-axis currents of DG units can be calculated as

$$\mathbf{I}_{\text{dvs}D} = \mathbf{G}_{\text{net}}\mathbf{E}_{\text{dvs}D} - \mathbf{B}_{\text{net}}\mathbf{E}_{\text{dvs}Q} \tag{6}$$

$$\mathbf{I}_{\text{dvs}Q} = \mathbf{B}_{\text{net}}\mathbf{E}_{\text{dvs}D} + \mathbf{G}_{\text{net}}\mathbf{E}_{\text{dvs}Q} \tag{7}$$

where

$$\mathbf{I}_{\text{dvs}D} = \begin{bmatrix} I_{\text{dvs}D1} \\ I_{\text{dvs}D2} \\ \vdots \\ I_{\text{dvs}Ds} \end{bmatrix}, \quad \mathbf{E}_{\text{dvs}D} = \begin{bmatrix} E_{\text{dvs}D1} \\ E_{\text{dvs}D2} \\ \vdots \\ E_{\text{dvs}Ds} \end{bmatrix}$$

$$\mathbf{I}_{\text{dvs}Q} = \begin{bmatrix} I_{\text{dvs}Q1} \\ I_{\text{dvs}Q2} \\ \vdots \\ I_{\text{dvs}Qs} \end{bmatrix}, \quad \mathbf{E}_{\text{dvs}Q} = \begin{bmatrix} E_{\text{dvs}Q1} \\ E_{\text{dvs}Q2} \\ \vdots \\ E_{\text{dvs}Qs} \end{bmatrix}.$$

In (6) and (7), $\mathbf{G}_{\text{net}}$ and $\mathbf{B}_{\text{net}}$ are the system conductance and susceptance matrices extracted from $\mathbf{Y}_{\text{net}}$; $E_{\text{dvs}Di}$ and $E_{\text{dvs}Qi}$ are the *DQ*-axis voltages of DVS *i* in the common reference frame; and $I_{\text{dvs}Di}$ and $I_{\text{dvs}Qi}$ are the *DQ*-axis currents of DVS *i* in the common reference frame. Normally, the reference frame of DG 1 is set as the common reference frame. As the real power sharing is always accurate with the droop control method, all the *D*-axis currents should be virtually equal. Assuming that all the *D*-axis voltages equal to the rated voltage of the microgrid and all the *Q*-axis voltages equal to zero, the *Q*-axis currents of DG units can be estimated accordingly. With the estimated vector $\mathbf{I}_{\text{dvs}Q}$, the reactive power sharing error of a given network can be evaluated.

As can be seen from the estimation method, the voltage magnitudes of DG units are assumed to be the same, and the capacity difference cannot be reflected. Thus, the estimation method is inapplicable for the system containing DG units with different capacities. This will affect the application scope of the virtual impedance optimization method.

B. Improved Reactive Power Estimation Method

To make up for the defects, an improved estimation method is proposed for the reactive power. The concepts of the equivalent network and the system admittance matrix $\mathbf{Y}_{\text{net}}$ are still used, but the estimation process for $\mathbf{I}_{\text{dvs}Q}$ is modified. As mentioned before, the reference frame of DVS 1 is set as the common reference frame; thus, the *Q*-axis voltage of DVS 1 should be zero. Then, (6) can be rewritten as

$$\mathbf{I}_{\text{dvs}D} = \mathbf{G}_{\text{net}}\mathbf{E}_{\text{dvs}D} - \mathbf{B}'_{\text{net}}\mathbf{E}'_{\text{dvs}Q} \tag{8}$$

where matrix $\mathbf{B}'_{\text{net}}$ is size of $s \times (s-1)$ and it is obtained from $\mathbf{B}_{\text{net}}$ by eliminating the first column. Similarly, vector $\mathbf{E}'_{\text{dvs}Q}$ is obtained from $\mathbf{E}_{\text{dvs}Q}$ by eliminating the first element $E_{\text{dvs}Q1}$. As the real power sharing is always accurate, the elements in $\mathbf{I}_{\text{dvs}D}$ should obey the following relationship:

$$I_{\text{dvs}Di} : I_{\text{dvs}Dj} = w_i : w_j \tag{9}$$

where

$$w_i = \frac{Q_{\max i}}{\sum_{i=1}^{s} Q_{\max i}}.$$

In (9), w_i and w_j are the power-sharing coefficients of DVS *i* and *j*, respectively. They are proportional to the DG capacities, and their sum equals to 1. Thus, the capacity differences are now reflected. Then, (8) can be transformed as

$$\mathbf{T}_{re}\mathbf{I}_{\mathrm{dvs}D} = \mathbf{T}_{re}\left(\mathbf{G}_{\mathrm{net}}\mathbf{E}_{\mathrm{dvs}D} - \mathbf{B'}_{\mathrm{net}}\mathbf{E'}_{\mathrm{dvs}Q}\right) = 0 \quad (10)$$

where

$$\mathbf{T}_{re} = \begin{bmatrix} w_2 & -w_1 & 0 & \cdots & 0 \\ w_3 & 0 & -w_1 & \cdots & 0 \\ \vdots & \vdots & \vdots & \ddots & \vdots \\ w_s & 0 & 0 & \cdots & -w_1 \end{bmatrix}_{(s-1)\times s}.$$

Then, the relationship between $\mathbf{E}_{\mathrm{dvs}D}$ and $\mathbf{E}_{\mathrm{dvs}Q}$ can be derived as

$$\mathbf{E}_{\mathrm{dvs}Q} = \mathbf{T}_{\mathrm{ed2eq}}\mathbf{E}_{\mathrm{dvs}D} \quad (11)$$

where

$$\mathbf{T}_{\mathrm{ed2eq}} = \mathbf{T}_{\mathrm{in}}(\mathbf{T}_{re}\mathbf{B'}_{\mathrm{net}})^{-1}\mathbf{T}_{re}\mathbf{G}_{\mathrm{net}}$$

and

$$\mathbf{T}_{\mathrm{in}} = \begin{bmatrix} 0 & 0 & \cdots & 0 \\ 1 & 0 & \cdots & 0 \\ 0 & 1 & \cdots & 0 \\ \vdots & \vdots & \ddots & \vdots \\ 0 & 0 & \cdots & 1 \end{bmatrix}_{s\times(s-1)}.$$

First, from the aspect of power sharing, the *Q*-axis voltages of DG units can be obtained. By substituting the vector $\mathbf{E}_{\mathrm{dvs}Q}$ in (7), the following equation can be obtained:

$$\mathbf{I}_{\mathrm{dvs}Q} = \mathbf{M}_{\mathrm{net}}\mathbf{E}_{\mathrm{dvs}D} \quad (12)$$

where

$$\mathbf{M}_{\mathrm{net}} = \mathbf{B}_{\mathrm{net}} + \mathbf{G}_{\mathrm{net}}\mathbf{T}_{\mathrm{ed2eq}}.$$

In this paper, $\mathbf{M}_{\mathrm{net}}$ is defined as the initial estimation matrix of the reactive power, which is determined by the parameters of the equivalent network and the capacities of DG units. Assuming that all the DG units have the same *D*-axis voltage, the reactive power of DG units can be estimated roughly, like the original estimation method did. However, the same voltage magnitude cannot reflect the capacity differences among DG units. Thus, the reactive power droop slopes are utilized here. According to (2), the reactive power and voltage magnitude of the DG unit should obey the following relationship:

$$Q_i = \frac{E_0 - E_i^*}{D_{qi}} \approx 1.5 I_{\mathrm{dvs}Qi}E_n \quad (13)$$

where E_n is the rated voltage of the microgrid. So the *Q*-axis current of each DG unit can be expressed as

$$I_{\mathrm{dvsQ}i} = t_i\left(E_0 - E_i^*\right) \quad (14)$$

where

$$t_i = \frac{2}{3E_n D_{qi}}.$$

After this, from the aspect of the droop controller, the vector $\mathbf{I}_{\mathrm{dvs}Q}$ can be expressed in another form as

$$\mathbf{I}_{\mathrm{dvs}Q} = E_0\mathbf{T}_2 + \mathbf{T}_1\mathbf{E}_{\mathrm{dvs}D} \quad (15)$$

where

$$\mathbf{T}_1 = \begin{bmatrix} t_1 & 0 & \cdots & 0 \\ 0 & t_2 & \cdots & 0 \\ \vdots & \vdots & \ddots & \vdots \\ 0 & 0 & \cdots & t_s \end{bmatrix}_{s\times s}, \quad \mathbf{T}_2 = \begin{bmatrix} t_1 \\ t_2 \\ \vdots \\ t_s \end{bmatrix}_{s\times 1}.$$

Based on (12) and (15), the vectors $\mathbf{E}_{\mathrm{dvs}D}$ and $\mathbf{I}_{\mathrm{dvs}Q}$ can be calculated accordingly as follows:

$$\mathbf{E}_{\mathrm{dvs}D} = E_0(\mathbf{M}_{\mathrm{net}} + \mathbf{T}_1)^{-1}\mathbf{T}_2 \quad (16)$$

$$\mathbf{I}_{\mathrm{dvs}Q} = E_0\mathbf{C}_Q \quad (17)$$

where

$$\mathbf{C}_Q = \mathbf{M}_{\mathrm{net}}(\mathbf{M}_{\mathrm{net}} + \mathbf{T}_1)^{-1}\mathbf{T}_2 = \begin{bmatrix} C_{q1} \\ C_{q2} \\ \vdots \\ C_{qs} \end{bmatrix}_{s\times 1}.$$

In (17), $\mathbf{C}_Q$ is a vector, which reflects the reactive power of different DG units. From the derived process of $\mathbf{C}_Q$, it can be seen that the reactive power state of a network is determined by the network parameters, virtual impedances, as well as the droop slopes. To observe the reactive power sharing state conveniently, the vector $\mathbf{C}_Q$ can be modified as follows:

$$\mathbf{C}_Q^* = \frac{1}{\sum_{i=1}^{s} C_{qi}}\mathbf{C}_Q = \begin{bmatrix} C_{q1}^* \\ C_{q2}^* \\ \vdots \\ C_{qs}^* \end{bmatrix}_{s\times 1}. \quad (18)$$

Then, by comparing C_{qi} and w_i, the reactive power sharing error of a single DG unit can be calculated as

$$\delta_{\mathrm{DG}i} = \left(C_{qi}^* - w_i\right) \times 100\%. \quad (19)$$

Then, the reactive power sharing error of a given network can be calculated accordingly as follows:

$$\delta_{\mathrm{net}j} = \sum_{i=1}^{s} |\delta_{\mathrm{DG}i}|. \quad (20)$$

In (20), $\delta_{\mathrm{net}j}$ reflects the reactive power sharing state of a given network, and it is determined by the equivalent network and droop control parameters. For example, if $\delta_{\mathrm{net}j}$ equals 50%, that means 50% of the load has not been well shared. The accuracy of the proposed estimation method will be validated through MATLAB simulation results in Section V. By improving the estimation method, the virtual impedance optimization method can be applied to the system containing different DG units. Normally, it would be better to regulate the virtual impedances rather than the droop slopes. Thus, if the virtual impedance can be controlled reasonably, the reactive power sharing performance of a microgrid will be improved.

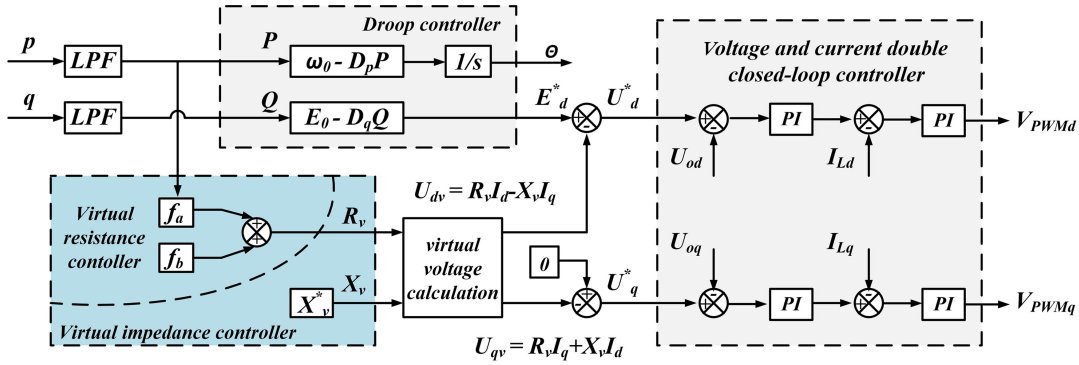

Fig. 5. Local control scheme based on the proposed method.

IV. Network Simplification for the Microgrid With More Nodes

A. Optimization Problem Design

To design an optimization problem for the reactive power sharing error elimination, there are mainly three basic issues that need to be noted: the optimization variable, the optimization objective, and the calculation amount.

1) Optimization Variable: Controller Parameters: In a low-voltage microgrid, virtual impedance is usually dominated by the virtual reactance. It is proved that the virtual resistance is more suitable for the reactive power regulation due to its stable regulating characteristic [20], [28]. So the virtual impedance controller here is designed as follows:

$$R_{vi} = f_{ai} P_i + f_{bi} \tag{21}$$

$$X_{vi} = X_v^* \tag{22}$$

where f_{ai} and f_{bi} are controller parameters, which need to be optimized through the optimization problem, and kept constant during the operation stage of the microgrid. As can be seen from (21) and (22), the virtual resistance is regulated by the real power of the DG unit, while the virtual reactance is constant. The control scheme of the DG unit with the proposed virtual impedance controller is depicted in Fig. 5.

As DG units locate in different positions of the microgrid and their network port characteristics are distinct, each controller will have different parameters (f_{ai} and f_{bi}). Finally, there will be $2 \times s$ optimization variables in the optimization problem.

2) Optimization Objective: The Average Reactive Power Sharing Error: After the optimization variables being determined, the corresponding optimization problem can be established, and it is important to choose a reasonable optimization objective. In [28], the global reactive power sharing error of the microgrid is set as the optimization objective. To reflect the reactive power sharing performance more clearly, the average reactive power sharing error is set as the optimization objective in this paper, which is defined as follows:

$$\delta_{\text{ave}} = \frac{1}{n_{\text{op}}} \delta_{\text{glb}} = \frac{1}{n_{\text{op}}} \sum_{j=1}^{n_{\text{op}}} \delta_{\text{net}j} \tag{23}$$

where n_{op} is the total number of the preset microgrid operation points; $\delta_{\text{net}j}$ is the reactive power sharing error of operation point

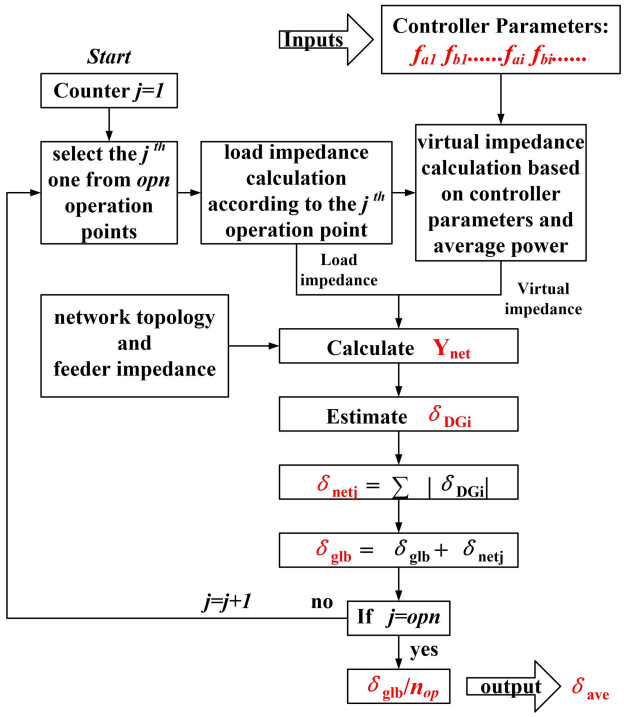

Fig. 6. Function $F_\delta(x)$. Calculation process of δ_{ave}.

j; δ_{glb} represents the global reactive power sharing error, which is obtained by accumulating the $\delta_{\text{net}j}$ value of each operation point; and δ_{ave} is the average reactive power sharing error, which reflects the comprehensive reactive power sharing performance of the microgrid. Compared with δ_{glb}, the value of δ_{ave} is more intuitive. For the microgrid, the value of δ_{ave} should be as small as possible. The calculation process of δ_{ave} is illustrated in Fig. 6, and the corresponding calculation function $F_\delta(x)$ needs to be established in MATLAB for the virtual impedance optimization.

3) Calculation Amount: Operation Point Number: For the fitness function $F_\delta(x)$, the calculation amount is mainly determined by the operation point number n_{op}, which can be calculated as

$$n_{\text{op}} = (n_p \times n_q)^m \tag{24}$$

where n_p and n_q are the real and reactive power operation point numbers for a single load, respectively. When the network node

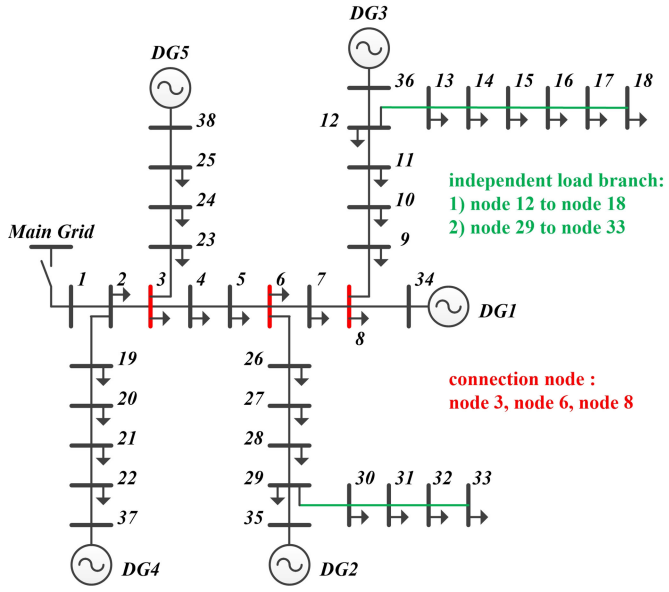

Fig. 7. Topology of the introduced 38-bus microgrid system.

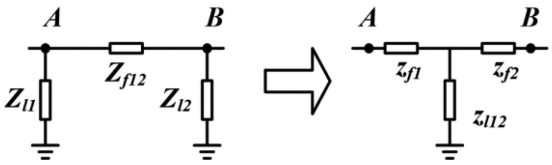

Fig. 8. Illustration for the Δ-Y transformation.

number m is small, the calculation amount of the optimization problem solving is acceptable. By solving the optimization problem, the average reactive power sharing error of the microgrid can be minimized. However, as the number m increases, the calculation amount will grow exponentially, making the proposed optimization method invalid.

B. Network Simplification

When a microgrid with more nodes is encountered, to limit the microgrid operation point number, a network simplification step is added before the optimization. To explain the network simplification method, the 38-bus microgrid system used in [29] is introduced here. The topology is shown in Fig. 7, with the related network parameters listed in Appendix A.

As can be seen from the figure, the microgrid contains 5 DG units and 32 loads. If each load is set with 3 real power operation points and 2 reactive power operation points, then the microgrid will totally have 6^{32} microgrid operation points, which is too large for the function $F_\delta(x)$. So, the network of the microgrid needs to be equivalently simplified. To achieve this, the well-known Δ-Y transformation can be utilized, which is illustrated in Fig. 8 and has the following formulae:

$$z_{f1} = \frac{Z_{f12}Z_{l1}}{Z_{f12}+Z_{l1}+Z_{l2}} \tag{25}$$

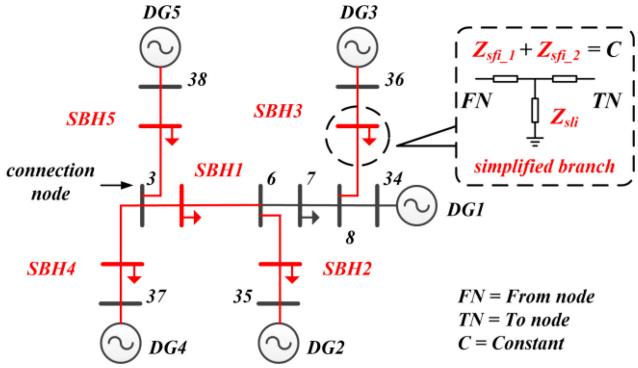

Fig. 9. Topology of the 38-bus system after the proposed simplification.

$$z_{l12} = \frac{Z_{l2}Z_{l1}}{Z_{f12}+Z_{l1}+Z_{l2}} \tag{26}$$

$$z_{f2} = \frac{Z_{f12}Z_{l2}}{Z_{f12}+Z_{l1}+Z_{l2}}. \tag{27}$$

When the Δ-Y transformation is applied to the power system, as the line impedance is much smaller than the load impedance, following relationships can be derived:

$$z_{f1}+z_{f2} \approx \frac{Z_{f12}Z_{l1}+Z_{f12}Z_{l2}}{Z_{l1}+Z_{l2}} = Z_{f12} \tag{28}$$

$$z_{l12} \approx \frac{Z_{l2}Z_{l1}}{Z_{l1}+Z_{l2}} = Z_{l2}||Z_{l1}. \tag{29}$$

It can be found that the new load after the transformation can be regarded as the parallel of the previous loads, and the total line impedance between the two nodes will remain unchanged. These characteristics will be utilized later in the generation of microgrid operation points. The simplification processes for a multinode topology are as follows: first, the independent load branch, such as the one from nodes 12 to 18, can be regarded as one load connected to the head node; second, the branch between DG unit node and connection node (the node with more than two feeders) is converted to the simplest form by using the Δ-Y transformation. With the above-mentioned two steps, the topology of the 38-bus system can be greatly simplified, as shown in Fig. 9.

In the figure, the red circuits indicate the simplified branches (SBH) of the network, and there are total five such branches in the simplified system. Z_{sfi} represents the total line impedance of SBH i, which is composed of Z_{sfi_1} and Z_{sfi_2}. According to (28), the value of Z_{sf_i} is definite. Thus, to describe an SBH, only two parameters are needed: Z_{sli} and Z_{sfi_1} (or Z_{sfi_2}). The load impedance Z_{sli} reflects the load amount, while Z_{sfi_1} reflects the load position. When the concept of SBH is introduced, the microgrid operation point number n_{op} can be greatly reduced. Each SBH has six operation points, just like the load does. Considering that there are five SBH and one load in the simplified network, the total microgrid operation point number will be 6^6, which is much smaller than its previous value.

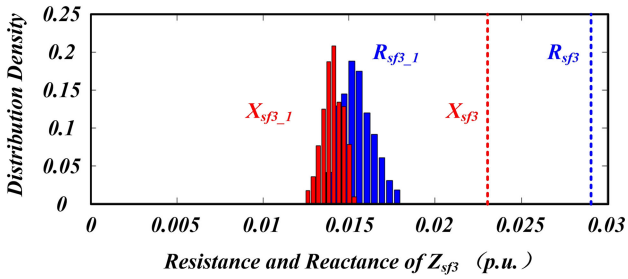

Fig. 10. Distribution of the load position parameters of SBH 3.

TABLE I
NETWORK PARAMETERS OF THE SIMPLIFIED SYSTEM

Branch		Line impedance of SBH (p.u.)		
Name	FN and TN	Load	Z_{fi_1}	Z_{sfi_2}
SBH 1	3 to 6	4, 5	$0.0035 + 0.0018j$	$0.0063 + 0.0050j$
SBH 2	35 to 6	6, 26–33	$0.0174 + 0.0166j$	$0.0097 + 0.0076j$
SBH 3	36 to 8	8–18	$0.0154 + 0.0141j$	$0.0135 + 0.0087j$
SBH 4	37 to 3	2, 19–22	$0.0215 + 0.0225j$	$0.0114 + 0.0098j$
SBH 5	38 to 3	3, 23–25	$0.0201 + 0.0184j$	$0.0063 + 0.0047j$
BH 1	6 to 8	7	$0.0012 + 0.0039j$	$0.0044 + 0.0015j$

Note: FN—from node and TN—to node.

TABLE II
CONSTRAINT CONDITION SETTING AND OPTIMIZATION RESULTS

Parameters		Value
Constraint condition	Condition 1	$-0.1 \le f_{ai} p_{\max i} + f_{bi} \le 0.2$
	Condition 2	$-0.5 \times 10^{-5} \le f_{ai} \le 0.5 \le 0.5 \times 10^{-5}$
	Condition 3	$-0.1 \le f_{bi} \le 0.2$
Optimization result	DG 1	$f_{a1} = -5.08 \times 10^{-6}$, $f_{b1} = 0.1952$
	DG 2	$f_{a2} = -4.46 \times 10^{-6}$, $f_{b2} = 0.0883$
	DG 3	$f_{a3} = 9.44 \times 10^{-6}$, $f_{b3} = -0.0648$
	DG 4	$f_{a4} = 1.50 \times 10^{-6}$, $f_{b4} = 0.1789$
	DG 5	$f_{a5} = -9.61 \times 10^{-6}$, $f_{b5} = 0.1985$

TABLE III
DG UNIT PARAMETERS USED IN MATLAB SIMULATION

Parameters		Value
Circuit parameters	*LCL*	$L_f = 1.5\,\text{mH}$, $C_f = 15\,\mu\text{F}$, $L_o = 0.3\,\text{mH}$
	Z_v	$R_v = 0.05\,\Omega$, $L_v = 0.1\,\Omega$
	Voltage	$f_0 = 50.125\,\text{Hz}$, $E_0 = 317.25\,\text{V}$
Droop slopes $S* = 25\,\text{kVA}$	DG 1 (1)	$D_{p1} = 0.5 \times 10^{-5}$, $D_{q1} = 0.5 \times 10^{-4}$
	DG 2 (1.5)	$D_{p2} = 0.333 \times 10^{-5}$, $D_{q2} = 0.333 \times 10^{-4}$
	DG 3 (1)	$D_{p3} = 0.5 \times 10^{-5}$, $D_{q3} = 0.5 \times 10^{-4}$
	DG 4 (0.5)	$D_{p4} = 1 \times 10^{-5}$, $D_{q4} = 1 \times 10^{-4}$
	DG 5 (1)	$D_{p5} = 0.5 \times 10^{-5}$, $D_{q5} = 0.5 \times 10^{-5}$

C. Operation Point Design for SBH

To design the operation point of the SBH rationally, related parameter analysis is carried out. Taking SBH 3 for example, after the first simplification step, the branch from node 36 to node 8 will have 5 loads, corresponding to 6^5 operation points. Each SBH operation point will correspond to a set of SBH parameters after the second simplification step, containing the load impedance (Z_{sli}) and the line impedance (Z_{sfi_1} or Z_{sfi_2}). The distribution of these parameters is shown in Fig. 10.

The total line impedance of SBH 3 is marked out in the figure. From the comparison between Z_{sf3_1} and Z_{sf3}, it can be seen that the position parameter Z_{sf3_1} only changes in a limited range. Thus, the load connection position of SBH 3 can be regarded as fixed. So, the average value of Z_{sf3_1} can be used to describe the load position approximately. This conclusion is also applicable to the other SBHs. Thus, a simplified network with exact line impedances can be obtained, with its corresponding parameters listed in Table I. By setting three real power operation points and two reactive power operation points to each SBH load, each SBH will have six operation points. The operation point setting can be found in Appendix B.

By setting the simplified system as the target system, the virtual impedance optimization method can be used now. The following steps are as usual: by establishing $F_\delta(x)$ as the fitness function and solving the optimization problem, the best values for those controller parameters can be obtained, which can minimize the average reactive power sharing error for the simplified system. The constraint conditions setting in the optimization as well as the optimization results are shown in Table II. The computation time for the optimization problem solving is associated with the number of microgrid operation points. When n_{op} is 6^5, it would take about 43 s to complete one optimization.

With the optimized controller parameters, the reactive power sharing performance of the simplified microgrid can be greatly improved. As the simplified system is an approximate model obtained based on the 38-bus system, the optimization results can be regarded as an approximate solution for the original system, which is also effective. This will be verified by MATLAB simulation results in the next section. Thus, the improved virtual impedance optimization method can be applied to the microgrid with more nodes.

V. SIMULATION VERIFICATION

To test the effectiveness of the improved virtual impedance optimization method, the 38-bus system depicted in Fig. 7 is established in MATLAB simulation. The parameters of the DG units are listed in Table III. The number in brackets represents the power capacity (p.u.) of the DG unit. The virtual impedance controller in each DG unit is standby in the beginning, and its controller parameters are obtained from the virtual impedance optimization. The optimization results are listed in Table II. Before the virtual impedance controllers work, fixed virtual impedances are added to improve the stability of the system.

A. Reactive Power Sharing Performance With the Proposed Method

The power-sharing performance of the simulated system is shown in Fig. 11. The dashed lines in the small figure illustrate the ideal power curves of DG units.

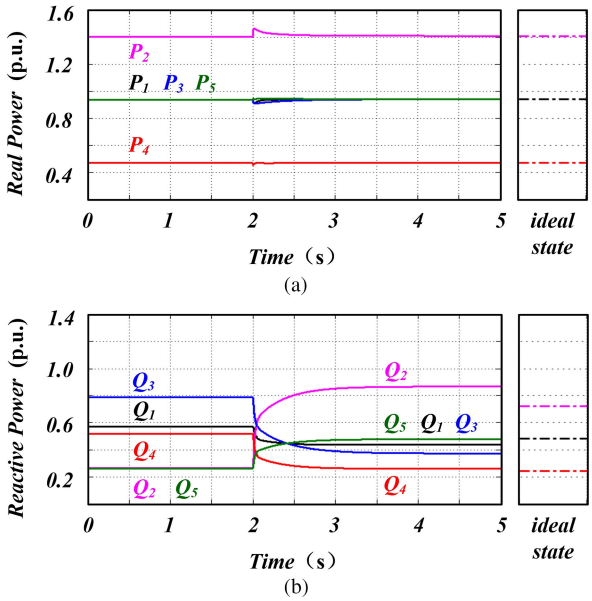

Fig. 11. Simulated power sharing performance of the 38-bus system. (a) Real power. (b) Reactive power.

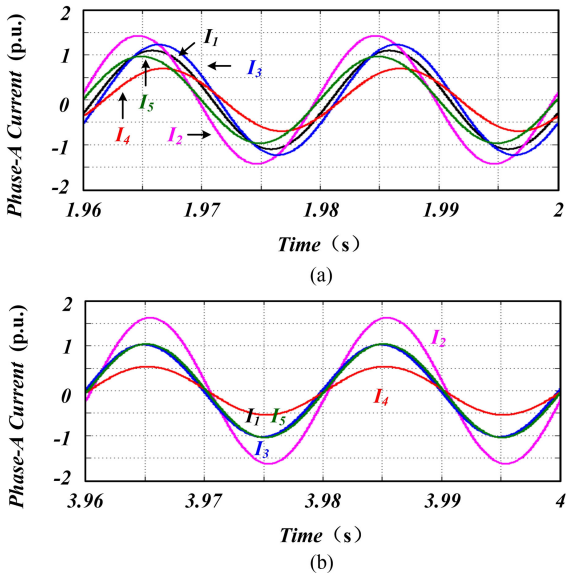

Fig. 12. Simulated current sharing performance of the 38-bus system. (a) With the conventional method. (b) With the proposed method.

In the simulation, each DG unit adopts the conventional droop control method. In the beginning, fixed virtual impedances are added; otherwise, the reactive power sharing performance could be even worse. As the figure shows, the real power sharing performance is satisfactory, but there are significant reactive power sharing errors. Before $t = 2$ s, DG 2 has the largest capacity but outputs the least reactive power. Instead, DG 3 outputs the most reactive power. This operation state deviates far from the expected state, which is harmful to the microgrid system. It will not only increase the transmission loss but also lead to the irrational utilization of DG units. At $t = 2$ s, the optimized virtual impedance controller in each DG unit is enabled. As can be seen from the figure, the real power sharing state keeps unchanged, while the reactive power sharing performance is greatly improved.

Fig. 12 shows the associated DG currents before and after the application of the optimized controllers. In an ideal state, DG units should output currents according to their capacities. However, this objective can hardly be achieved with the conventional method. As can be seen from Fig. 12(a), DG 1, 3, and 5 have different current phases and magnitudes, although they have the same capacity. The current sharing performance is greatly improved after the virtual impedance controllers start to work. As Fig. 12(b) shows, each DG unit can output current as expected. Although there are still some reactive power sharing errors in the system, their impact on the current sharing performance is small.

The simulation results of the reactive power can be used to verify the effectiveness of the improved estimation method. By establishing matrices $\mathbf{M}_{\text{net}}$, $\mathbf{T}_1$, and $\mathbf{T}_2$, the reactive power of each DG unit can be estimated. The estimation and simulation results are compared in Table IV. As the original estimation method cannot estimate the system containing DG units with different capacities, it will not be shown here.

TABLE IV
SIMULATION AND ESTIMATION RESULTS

Parameters		Simulation results (p.u.)	Estimation results (p.u.)
System with the conventional method	Q_1	0.5722	0.5776
	Q_2	0.2658	0.2658
	Q_3	0.7875	0.8087
	Q_4	0.5193	0.5138
	Q_5	0.2606	0.2549
	$\delta_{\text{net}j}$	0.5623	0.5698
System with the proposed method	Q_1	0.4811	0.442
	Q_2	0.8672	0.8730
	Q_3	0.3724	0.4092
	Q_4	0.2594	0.2555
	Q_5	0.4778	0.4756
	$\delta_{\text{net}j}$	0.1339	0.1192

As Table IV shows, the improved estimation method can well reflect the reactive power sharing state of the network, and the estimation errors are acceptable. Compared with the simulation results, the calculation time of estimation results is much shorter. So it is feasible to use the estimation method in the calculation of δ_{ave}, which serves the parameter optimization of the virtual impedance controller. It can also be used to test the reactive power sharing performance of different reactive power sharing strategies.

B. Reactive Power Sharing Performance Under Different Microgrid Operation Points

Above-mentioned simulation results have proved that the optimization method can work well under a certain network, which only corresponds to one microgrid operation point. However,

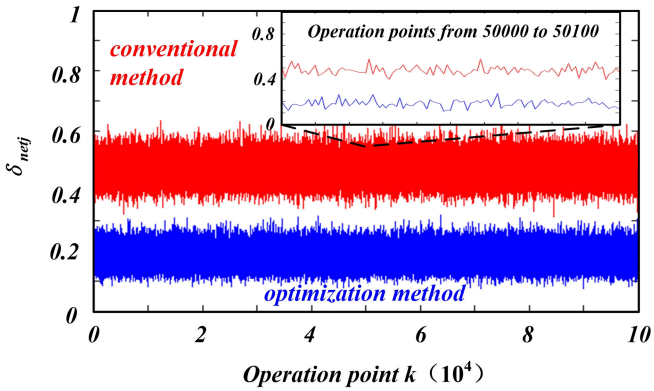

Fig. 13. $\delta_{\text{net}j}$ calculation results of the generated 10^5 operation points: red points for the fixed virtual impedance method and blue for the improved virtual impedance optimization method.

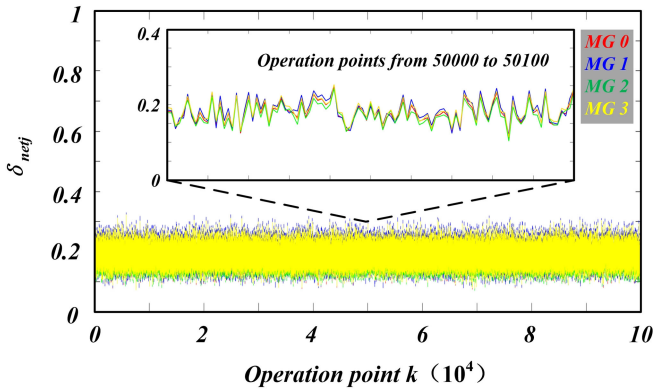

Fig. 14. Reactive power sharing performances of different microgrids with the same virtual impedance controllers.

more operation points are required to demonstrate the effectiveness of the optimization method. As mentioned before, the 38-bus system totally has 6^{32} operation points. It is impractical to calculate the $\delta_{\text{net}j}$ value of each operation point. Thus, 10^5 operation points are generated randomly for the reactive power sharing performance comparison between the fixed virtual impedance method and the virtual impedance optimization method. The $\delta_{\text{net}j}$ values of the generated operation points are shown in Fig. 13.

From the comparison shown in Fig. 13, it can be seen that the system with the optimization method has a much better reactive power sharing performance. The $\delta_{\text{net}j}$ values with the conventional method are always higher than those with the optimization method, and most of them have exceeded 40%. While with the optimization method, the $\delta_{\text{net}j}$ values are limited under 30%. That means more than half of the reactive power sharing errors are eliminated through the virtual impedance optimization. Overall, the reactive power sharing errors become acceptable after the optimization. It is worth noting that the optimized controller parameters are obtained from the simplified system. However, they are equally valid in the 38-bus system as the result shows.

C. Reactive Power Sharing Performance in Mismatched Systems

To test the fault-tolerant capability of the proposed method, the optimized virtual impedance controllers designed for the original target system will be applied to several new microgrid systems. These new systems are created from the original system by changing the feeder impedances. The reactive power sharing performances of these different microgrids that apply the same virtual impedance controllers are compared in Fig. 14.

In Fig. 14, MG 0 represents the original 38-bus microgrid system. The line impedances in MG 1 are increased by 15%, and the line impedances in MG 2 are decreased by 15%. In MG 3, the line impedances are changed randomly between 85% and 115%. As can be seen from the figure, the virtual impedance controllers designed for the original target system are also suitable for the newly created systems. Most $\delta_{\text{net}j}$ values are still limited under 30%, which is acceptable compared with the performance of the conventional method. This result well proves that the proposed method has some fault-tolerant capability to the line impedance errors.

VI. Conclusion

The virtual impedance optimization method enables the wireless reactive power sharing control of the microgrid. Compared with the communication based reactive power sharing strategy, the optimization method based control strategy is fully distributed and independent of communication network. It can conveniently help the existing microgrid improving the reactive power sharing performance. However, the original optimization method has not considered the capacity differences of DG units as well as the microgrid with more nodes. Thus, an enhanced virtual impedance optimization method is hereby proposed to solve the above-mentioned issues. First, the reactive power estimation method, as the key technique of the optimization method, is modified by introducing reactive power droop slopes. Second, a network simplification step is added before the optimization, which reduces the microgrid operation points but without affecting the optimization effect. Through the above-mentioned improvements, the application scope of the optimization method is largely extended. Through MATLAB simulation results, the effectiveness and feasibility of the improved optimization method have been well proved. For an actual microgrid, if loads operate regularly, the operation points can be designed more specifically; thus, the virtual impedance optimization method can be more effective.

Appendix

A. Network Parameters

The network parameters of the 38-bus system reference to [29]. The rated capacity S^* set in this paper is 25 kVA, and the rated voltage is set to 380 V.

TABLE V
NETWORK PARAMETERS OF THE 38-BUS SYSTEM AND LOAD OPERATION POINTS SET IN THE SIMULATION

Line impedance				Load on TN in the simulation	
FN	TN	R (p.u.)	X (p.u.)	P (p.u.)	Q (p.u.)
1	2	0.000574	0.000293	0.06	0.12
2	3	0.00307	0.001564	0.12	0.06
3	4	0.002279	0.001161	0.18	0.18
4	5	0.002373	0.001209	0.18	0.18
5	6	0.0051	0.004402	0.18	0.06
6	7	0.001166	0.003853	0.06	0.12
7	8	0.00443	0.001464	0.18	0.06
8	9	0.006413	0.004608	0.18	0.06
9	10	0.006501	0.004608	0.18	0.06
10	11	0.001224	0.000405	0.18	0.06
11	12	0.002331	0.000771	0.18	0.06
12	13	0.009141	0.007192	0.18	0.06
13	14	0.003372	0.004439	0.18	0.06
14	15	0.00368	0.003275	0.18	0.06
15	16	0.004647	0.003394	0.18	0.06
16	17	0.008026	0.010716	0.18	0.06
17	18	0.004558	0.003574	0.18	0.06
2	19	0.001021	0.000974	0.06	0.12
19	20	0.009366	0.00844	0.06	0.12
20	21	0.00255	0.002979	0.06	0.12
21	22	0.004414	0.005836	0.06	0.12
3	23	0.004414	0.005836	0.12	0.06
23	24	0.005592	0.004415	0.12	0.06
24	25	0.005579	0.004366	0.12	0.06
6	26	0.001264	0.000644	0.18	0.06
26	27	0.00177	0.000901	0.18	0.06
27	28	0.006594	0.005814	0.18	0.06
28	29	0.005007	0.004362	0.18	0.06
29	30	0.00316	0.00161	0.18	0.06
30	31	0.006067	0.005996	0.18	0.06
31	32	0.001933	0.002253	0.18	0.06
32	33	0.002123	0.003301	0.18	0.06
8	34	0.012453	0.012453	0	0
29	35	0.012453	0.012453	0	0
12	36	0.012453	0.012453	0	0
22	37	0.012453	0.012453	0	0
25	38	0.012453	0.012453	0	0

B. Operation Point Setting for Each SBH

In this paper, each load and each SBH are set with three real power operation points and two reactive power operation points. The load range of an SBH is associated with the load number before the simplification.

TABLE VI
OPERATION POINT SETTING FOR THE 38-BUS SYSTEM

		Real and reactive power operation points
Original system	Load 1–32	$P = [0.06\ 0.12\ 0.18]$ $Q = [0.06\ 0.12]$
Simplified system	SBH 1	$P = [0.12\ 0.24\ 0.36]$ $Q = [0.12\ 0.24]$
	SBH2	$P = [0.54\ 0.98\ 1.62]$ $Q = [0.54\ 0.98]$
	SBH 3	$P = [0.66\ 1.32\ 1.98]$ $Q = [0.66\ 1.32]$
	SBH 4	$P = [0.30\ 0.60\ 0.90]$ $Q = [0.30\ 0.60]$
	SBH 5	$P = [0.24\ 0.48\ 0.72]$ $Q = [0.24\ 0.48]$

REFERENCES

[1] M. A. Zamani, T. Sidhu, and A. Yazdani, "Investigations into the control and protection of an existing distribution network to operate as a microgrid: A case study," *IEEE Trans. Ind. Electron.*, vol. 61, no. 4, pp. 1904–1915, Apr. 2014.

[2] I. U. Nutkani, P. C. Loh, and F. Blaabjerg, "Droop scheme with considering of operating cost," *IEEE Trans. Power Electron.*, vol. 29, no. 3, pp. 1047–1052, Mar. 2014.

[3] C. N. Rowe, T. J. Summers, R. E. Betz, D. J. Cornforth, and T. G. Moore, "Arctan power-frequency droop for improved microgrid stability," *IEEE Trans. Power Electron.*, vol. 28, no. 8, pp. 3747–3759, Aug. 2013.

[4] Y. Han, H. Li, P. Shen, E. A. A. Coelho, and J. M. Guerrero, "Review of active and reactive power sharing strategies in hierarchical controlled microgrids," *IEEE Trans. Power Electron.*, vol. 32, no. 3, pp. 2427–2451, Mar. 2017.

[5] J. M. Guerrero, L. G. Vicuna, J. Matas, M. Castilla, and J. Miret, "Output impedance design of parallel-connected UPS inverters with wireless load sharing control," *IEEE Trans. Ind. Electron.*, vol. 52, no. 4, pp. 1126–1135, Aug. 2005.

[6] J. M. Guerrero, L. G. Vicuna, J. Matas, M. Castilla, and J. Miret, "A wireless controller to enhance dynamic performance of parallel inverters in distributed generation systems," *IEEE Trans. Power Electron.*, vol. 19, no. 4, pp. 1205–1213, Sep. 2004.

[7] J. Kim, J. M. Guerrero, P. Rodriguez, R. Teodorescu, and K. Nam, "Mode adaptive droop control with virtual output impedances for an inverter based flexible ac microgrid," *IEEE Trans. Power Electron.*, vol. 26, no. 3, pp. 689–701, Mar. 2011.

[8] W. Yao, M. Chen, J. Matas, J. M. Guerrero, and Z. M. Qian, "Design and analysis of the droop control method for parallel inverters considering the impact of the complex impedance on the power sharing," *IEEE Trans. Ind. Electron.*, vol. 58, no. 2, pp. 576–588, Feb. 2011.

[9] J. M. Guerrero, J. Matas, L. G. De Vicuna, M. Castilla, and J. Miret, "Decentralized control for parallel operation of distributed generation inverters using resistive impedance," *IEEE Trans. Power Electron.*, vol. 54, no. 2, pp. 994–1004, Apr. 2007.

[10] Y. W. Li and C. N. Kao, "An accurate power control strategy for power electronics-interfaced distributed generation units operation in a low voltage multibus microgrid," *IEEE Trans. Power Electron.*, vol. 24, no. 12, pp. 2977–2988, Dec. 2009.

[11] J. He, Y. W. Li, J. M. Guerrero, F. Blaabjerg, and J. C. Vasquez, "An islanding microgrid power sharing approach using enhanced virtual impedance control scheme," *IEEE Trans. Power Electron.*, vol. 28, no. 11, pp. 5272–5282, Nov. 2013.

[12] Y. X. Zhu, F. Zhuo, F. Wang, B. Q. Liu, and Y. J. Zhao, "A wireless load sharing strategy for islanded microgrid based on feeder current sensing," *IEEE Trans. Power Electron.*, vol. 30, no. 12, pp. 6706–6719, Dec. 2015.

[13] J. W. He and Y. W. Li, "An enhanced microgrid load demand sharing strategy," *IEEE Trans. Power Electron.*, vol. 27, no. 9, pp. 3984–3995, Sep. 2012.

[14] H. Han, Y. Liu, Y. Sun, M. Su, and J. M. Guerrero, "An improved droop control strategy for reactive power sharing in islanded microgrid," *IEEE Trans. Power Electron.*, vol. 30, no. 6, pp. 3133–3141, Jun. 2015.

[15] Y. X. Zhu, F. Zhuo, B. Q. Liu, and H. Yi, "An enhanced load power sharing strategy for low-voltage microgrids based on inverse-droop control method," in *Proc. Int. Power Electron. Conf.*, Hiroshima, Japan, 2014, pp. 3546–3552.

[16] T. L. Vandoorn, J. D. M. De Kooning, B. Meersman, and L. Vandevelde, "Communication-based secondary control in microgrids with voltage based droop control," in *Proc. IEEE Transm. Distrib. Conf. Expo.*, 2012, pp. 1–6.

[17] M. Savaghebi, A. Jalilian, J. C. Vasquez, and J. M. Guerrero, "Secondary control scheme for voltage unbalanced compensation in an islanded droop controlled microgrid," *IEEE Trans. Smart Grid*, vol. 3, no. 2, pp. 797–807, Jun. 2012.

[18] H. Mahmood, D. Michaelson, and J. Jiang, "Accurate reactive power sharing in an islanded microgrid using adaptive virtual impedances," *IEEE Trans. Power Electron.*, vol. 30, no. 3, pp. 1605–1617, Mar. 2015.

[19] Y. Zhang and H. Ma, "Analysis of networked control schemes and data processing method for parallel inverters," *IEEE Trans. Ind. Electron.*, vol. 61, no. 4, pp. 1834–1844, Apr. 2014.

[20] Y. X. Zhu, B. Q. Liu, F. Wang, F. Zhuo, and Y. J. Zhao, "A virtual resistance based reactive power sharing strategy for networked microgrid," in *Proc. IEEE 9th Int. Conf. Power Electron. ECCE Asia*, Jul. 2015, pp. 1564–1572.

[21] H. G. Zhang, S. Kim, Q. Y. Sun, and J. G. Zhou, "Distributed adaptive virtual impedance control for accurate reactive power sharing based on consensus control in microgrids," *IEEE Trans. Smart Grid*, vol. 6, no. 6, pp. 3006–3019, Nov. 2015.
[22] F. Guo, C. Wen, J. Mao, and Y. D. Song, "Distributed secondary voltage and frequency restoration control of droop-controlled inverter based microgrids," *IEEE Trans. Ind. Electron.*, vol. 62, no. 7, pp. 4355–4364, Jul. 2015.
[23] Q. Shafiee, J. M. Guerrero, and J. C. Vasquez, "Distributed secondary control for islanded microgrids-A novel approach," *IEEE Trans. Power Electron.*, vol. 29, no. 2, pp. 1018–1031, Feb. 2014.
[24] J. Zhou, S. Kim, H. Zhang, Q. Sun, and R. Han, "Consensus-based distributed control for accurate reactive, harmonic and imbalance power sharing in microgrids," *IEEE Trans. Smart Grid*, to be published, doi: 10.1109/TSG.2016.2613143.
[25] J. W. Simpson-Porco, Q. Shafiee, F. Dorfler, J. C. Vasquez, J. M. Guerrero, and F. Bullo, "Secondary frequency and voltage control of islanded microgrids via distributed averaging," *IEEE Trans. Ind. Electron.*, vol. 58, no. 1, pp. 7025–7038, Nov. 2016.
[26] R. Han, L. Meng, G. Ferrari-Trecate, E. A. A. Coelho, J. C. Vasquez, and J. M. Guerrero, "Containment and consensus-based distributed coordination control to achieve bounded voltage and precise reactive power sharing in islanded ac microgrids," *IEEE Trans. Ind. Appl.*, vol. 53, no. 6, pp. 5187–5199, Nov./Dec. 2017.
[27] V. Nasirian, Q. Shafiee, J. M. Guerrero, F. L. Lewis, and A. Davoudi, "Droop-free distributed control for ac microgrid," *IEEE Trans. Power Electron.*, vol. 31, no. 2, pp. 1600–1617, Feb. 2016.
[28] Y. X. Zhu, F. Zhuo, F. Wang, B. Q. Liu, R. F. Gou, and Y. J. Zhao, "A virtual impedance optimization method for reactive power sharing in networked microgrid," *IEEE Trans. Power Electron.*, vol. 31, no. 4, pp. 2890–2904, Apr. 2016.
[29] C. D. Li, S. K. Chaudhary, M. Savaghebi, J. C. Vasquez, and J. M. Guerrero, "Power flow analysis for low-voltage ac and dc microgrids considering droop control and virtual impedance," *IEEE Trans. Smart Grid*, vol. 8, no. 6, pp. 2754–2764, Nov. 2017.

Yixin Zhu (S'11–M'17) received the B.S., M.S., and Ph.D. degrees in electrical engineering from Xi'an Jiaotong University, Xi'an, China, in 2009, 2011, and 2015, respectively.

In 2016, he joined Jiangnan University, Wuxi, China, as a Lecturer. He is currently with the School of Internet of Things, Jiangnan University. His research interests include the design, control, and application of the high-power active power filter, the photovoltaic grid-connected inverter, and also the modeling, analysis, and power management of the microgrid.

Qigao Fan (M'18) received the B.S. and M.S. degrees in control and instrumentation and the Ph.D. degree in mechatronic engineering from the China University of Mining Technology, Xuzhou, China, in 2008, 2010, and 2013, respectively.

In 2013, he joined Jiangnan University, Wuxi, China, as a Lecturer. He is currently an Associate Professor of electrical engineering with the School of Internet of Things (IoT), Jiangnan University. His research interests include indoor localization, robotics, intelligent casting, wireless microelectromechanical system based technologies, and IoT sensor technology.

Baoquan Liu (M'17) was born in Hebei, China, in 1987. He received the B.S. degree in electrical engineering from the Harbin Institute of Technology, Harbin, China, in 2009, and the M.S. and Ph.D. degrees from Xi'an Jiaotong University, Xi'an, China, in 2012 and 2015, respectively.

He is currently an Associate Professor with the School of Electrical and Information Engineering, Shaanxi University of Science and Technology, Xi'an, China. His research interests include system design and power flow control of dc and ac microgrids using hybrid energy storage.

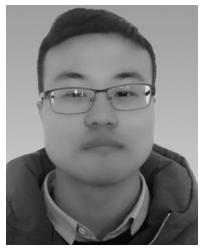

Tao Wang received the B.S. degree in automation from Yangzhou University, Yangzhou, China, in 2016. He is currently working toward the M.S. degree in electrical engineering at Jiangnan University, Wuxi, China.

His research interests include energy management of the microgrid and electric vehicle charging technology.